

Effects of stereoisomeric structure and bond location on the ignition and reaction pathways of  
hexenes

Cesar L. Barraza-Botet<sup>1</sup>, Changpeng Liu<sup>2,\*</sup>, John H. Kim<sup>3</sup>, Scott W. Wagnon<sup>4</sup>, Margaret S. Wooldridge<sup>3,5,6</sup>

<sup>1</sup>Energy, Materials and Environment Laboratory, Universidad de la Sabana, Chía 250001, Colombia

<sup>2</sup>State Key Laboratory of Automotive Safety and Energy, Tsinghua University, Beijing 100084, China

<sup>3</sup>Department of Mechanical Engineering, University of Michigan, Ann Arbor, MI 48109, USA

<sup>4</sup>Lawrence Livermore National Laboratory, Livermore, CA 94550, USA

<sup>5</sup>Aerospace Engineering, University of Michigan, Ann Arbor, MI 48109, USA

\*Current affiliation: Powertrain Engineering R&D Institute, Chongqing Changan Automotive Co. Ltd., 226 Liangjiang Road, 401133 Chongqing, China

<sup>6</sup>Corresponding author, mswool@umich.edu

**Abstract:** The current work presents new experimental autoignition and speciation data on the two cis-hexene isomers: cis-2-hexene and cis-3-hexene. The new data provide insights on the effects of carbon-carbon double bond location and stereoisomeric structures on ignition delay times and reaction pathways for linear hexene isomers. Experiments were performed using the University of Michigan rapid compression facility to determine ignition delay times from pressure-time histories.

This is the author manuscript accepted for publication and has undergone full peer review but has not been through the copyediting, typesetting, pagination and proofreading process, which may lead to differences between this version and the [Version of Record](#). Please cite this article as [doi: 10.1002/kin.21442](https://doi.org/10.1002/kin.21442).

This article is protected by copyright. All rights reserved.

Stoichiometric ( $\phi = 1.0$ ) mixtures at dilution levels of inert gas to  $O_2 = 7.5:1$  (mole basis) were investigated at an average pressure of 11 atm and temperatures from 809 to 1052 K. Speciation experiments were conducted at  $T = 900$  K for the two cis-hexene isomers, where fast-gas sampling and gas chromatography were used to identify and quantify the two cis-hexene isomers and stable intermediate species. The ignition delay time data showed negligible sensitivity to the location of the carbon-carbon double bond and the stereoisomeric structure (cis-trans), and the species data showed no correlation with stereoisomeric structure, but there was strong correlation of some of the measured species with the location of the double bond in the hexene isomer. In particular, 2-hexene showed strong selectivity to propene, acetaldehyde, and 1,3-butadiene, and 3-hexene showed selectivity to propanal. Model predictions of ignition delay times were in excellent agreement with the experimental data. There was generally good agreement for the model predictions of the species data for 2-hexene; however, the mechanism over-predicted some of the small aldehyde ( $C_2-C_4$ ) species for 3-hexene. Reaction pathway analysis indicates the hexenes are almost exclusively consumed by H-atom abstraction reactions at the conditions studied ( $P=11$  atm,  $T> 900$  K), and not by C3-C4 scission as observed in high temperature ( $>1300$  K) hexene ignition studies. Improved estimates for 3-hexene + OH reactions may improve model predictions for the species measured in this work.

**Keywords:** hexene isomers, ignition and species measurements, cis and trans isomers

## 1. Introduction

Biodiesel fuels are promising alternatives to petroleum-derived fuels, particularly if biodiesel fuel can be produced economically at scale from feedstock that does not compete with food resources. The unsaturated esters found in biodiesel fuels are often *cis*-isomers of the compounds [1]. There are few studies which have examined the combustion behavior of stereoisomeric (*cis-trans*) olefins, and hence the objective of this study was to identify and quantify similarities and differences in *cis* and *trans* isomers of the important combustion species hexene. The different isomer structures considered in this study are shown in **Fig. 1**.

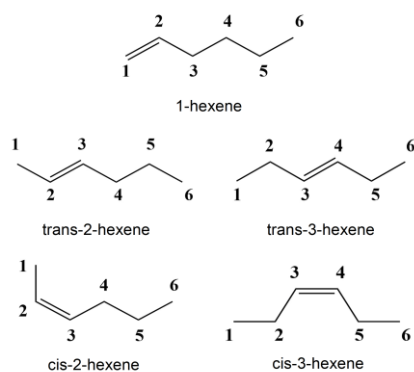


**Figure 1.** Structures of the linear hexene isomers

The hexene isomers not only provide an opportunity to study *cis-trans* effects on combustion chemistry; they are also important due to the role they play in combustion. 1-hexene is frequently used in multi-component fuel mixtures to represent linear alkenes found in real fuels [2], and most of the previous combustion studies of the hexene isomers have focused on 1-hexene. Some of the earliest studies provided rate estimates for 1-hexene oxidation [3] and 1-hexene thermal

decomposition, and the studies identified the dominant thermal decomposition pathways at combustion temperatures ( $T > 900$  K) as competition between fission of the C3 and C4 bond to form allyl and propyl radicals ( $1\text{-C}_6\text{H}_{12} \rightarrow \text{C}_3\text{H}_5 + \text{C}_3\text{H}_7$ ) and the retro-ene reaction ( $1\text{-C}_6\text{H}_{12} \rightarrow 2\text{C}_3\text{H}_6$ ) [4,5]. More recent studies by Yahyaoui et al. [6], indicated the dominant fuel consumption pathway during ignition at 1300 K was by thermal decomposition (>50%) via the carbon C3-C4 scission reaction. The retro-ene reaction was relatively inactive (1% fuel consumption), and the role of OH and H reactions with  $1\text{-C}_6\text{H}_{12}$  was responsible for about 22% of the fuel consumption. At 1700 K, thermal decomposition to form allyl and propyl radicals was the dominant fuel consumption pathway. Fan et al. [7] also found the allylic C-C bond dissociation to be the most important reaction during high temperature pyrolysis ( $T \sim 1200$  K), while during high-temperature oxidation, C-C bond dissociation and H-atom abstraction by radicals were both important fuel consumption pathways.

Regarding 2- and 3-hexene, prior work has exclusively considered the trans isomers. In one of the earliest studies comparing hexene isomer reactivity, Vanhove et al. [8] measured the auto-ignition behavior of 1-hexene, trans-2-hexene, and trans-3-hexene at pressures of 6.8 to 8.5 bar and temperatures of 630 to 850 K using a rapid compression machine. The authors found the autoignition behavior was a strong function of the location of the double bond at the intermediate temperatures studied, where 1-hexene was the most reactive (smallest ignition delay times), trans-3-hexene was the least reactive (highest ignition delay times) and trans-2-hexene exhibited intermediate reactivity.

In Mehl et al. [9], a comprehensive reaction mechanism was developed to represent the differences in the linear hexene isomers: 1-hexene, trans-2-hexene and trans-3-hexene. They

confirmed the dominant reaction pathway for all three isomers at high temperatures is scission of an allylic C–C bond, and the subsequent reactivity of the fuel fragments dictates the overall reactivity of the isomers. Based in part on the lack of any experimental data on the n-hexene isomers at high-temperatures, later work by Mehl et al. [10] compared the effects of the position of the double bond on the ignition properties of the linear hexene isomers at low (650–850 K) and (1000–1400 K) high temperatures. In addition to new experimental data, the authors proposed a new reaction mechanism, which included more detailed reaction pathways for the hexene isomers than their earlier work [9]. At low temperatures, longer alkyl chains yielded shorter ignition delay times, as found in Vanhove et al. [8], while at about 1000 K the authors found the reactivity was determined by the radicals formed by the  $\beta$ -scission decompositions of the resonance-stabilized radicals. At high temperatures above 1400 K, the oxidation process was driven by the initiation reaction of allylic C–C bond scission.

Bounaceur et al. [11] used quantum calculations to consider cis and trans transition states for the linear hexene isomers. They found the alkenes formed alkenyl and alkenyl peroxy radicals that can undergo isomerization pathways and that it was important to consider cis–trans conformations. The authors quantified the main channels of reaction of the hexene isomers in air at 750 K and 9 atm and found OH addition dominated 1-hexene fuel consumption, while H-atom abstraction/combination dominated the consumption of trans-3-hexene at the same conditions. While the reaction mechanism developed by Bounaceur et al. [11] represented the 1-hexene experimental data well, formation of butanal from trans-2-hexene and propanal from trans-3-hexene were underestimated. They confirmed butanal and propanal, and others, are sentinel intermediates

with strong correlation with the different trans-hexene isomers. The role of the cis and trans transition states identified by Bounaceur et al. [11] for the linear hexene indicates the cis and trans isomers may exhibit differences in reactivity and reaction pathways at combustion conditions.

Battin-Leclerc et al. [12] expanded the experimental data comparing products from 1-hexene, trans-2-hexene and trans-3-hexene at temperatures ranging from 500 to 1100 K at approximately atmospheric pressure. The results confirmed 2-hexene selectivity at 625 K to produce butanal and 3-hexene to produce propanal. The authors also found production of these intermediates was dramatically reduced at 825 K.

In the rapid compression facility (RCF) study by Wagnon et al. [13], the authors compared ignition delay times of the linear hexenes at intermediate temperatures from 840 K to 1090 K with  $P = 11$  atm, and the study included measurements of 13 intermediate species at  $T = 900$  K and  $P = 11$  atm. The ignition data were well represented using a detailed reaction mechanism developed at Lawrence Livermore National Laboratories (LLNL) by Mehl et al. [2], and the species measurements and predictions provided insights on the differences in the reaction pathways of the isomers. For example, the experimental data indicated a longer alkyl chain promotes significantly higher propene production (a factor of  $\sim 5$  increase in propene comparing trans-3-hexene with 1-hexene at times close to ignition), and this trend was well predicted by the mechanism simulations for the three isomers. Additionally, the experimental data showed trans-3-hexene selectivity to propanal production, as was found by Battin-Leclerc et al. [12] at 625 K. However, while the time histories for propanal were well-predicted for 1-hexene and trans-2-hexene, propanal was significantly overpredicted (by at least one order of magnitude) for trans-3-hexene. This is contrary to the

reaction mechanism predictions by Bounaceur et al. [11] who found the model simulations underpredicted the formation of the unsaturated aldehyde propanal from trans-3-hexene.

The most recent experimental and computational work on the linear hexene isomers is from Yang et al. [14,15,16] who studied ignition characteristics of trans-3-hexene behind reflected shock waves at high temperatures and equivalence ratios ranging from 0.5 to 1.5. They found the Mehl et al. [2] mechanism failed to capture the pressure dependence at high temperature. They proposed modifications to the Mehl et al. [2] mechanism and conducted reaction pathway analysis showing that initiation reactions dominated the trans-3-hexene system in high-temperature regions. In a companion study, Yang et al. [15] studied the ignition behavior of 1-hexene and trans-2-hexene using reflected shock waves at  $P=1.2-10$  atm and  $T=1020-1900$  K. They found the trans-2-hexene isomer to be more reactive than 1-hexene and proposed the difference was due to stabilization of intermediate radicals formed by 1-hexene. In their computational study, Yang et al. [16] used ab initio transition state modeling to evaluate the rates and branching fractions of the trans-3-hexene + OH reactions. The modeling results showed the OH addition to trans-3-hexene was the most important reaction pathway for temperatures  $<450$  K. For temperatures above 1000 K, H-atom abstraction (with over 70% removal of the allylic H atom) was the dominant reaction path. At intermediate temperatures, the results indicated both reaction systems were important.

To our knowledge no studies exist on the combustion and ignition behavior of cis-isomers of hexenes, particularly at low temperatures ( $<1000$  K) where the dominant reaction pathways can change dramatically as seen in the prior studies. The previous trans-hexene studies provide an excellent foundation for comparison, particularly of overall reactivity and of sentinel intermediate

species like propanal. Moreover, it is unclear based on the available literature whether proposed biodiesel surrogates should consist of cis or trans (or blends of both) compounds to appropriately capture the combustion kinetics of real biodiesel fuels, and studies of both isomeric forms will provide insight into appropriately representing biodiesel chemistry. Consequently, the objective of the current study was to quantify the ignition delay times and measure key intermediate species formed during ignition of the cis-hexene isomers for comparison with existing data on the trans-hexene isomers.

## 2. Experimental Approach

The University of Michigan (UM) RCF was utilized to carry out the ignition and speciation experiments for the two linear isomers of cis-hexene. A detailed description of the UM RCF can be found in Wagnon et al. [13]. The operation and key characteristics of the facility are briefly reviewed here. The UM RCF is a free piston/cylinder device used to create rapidly high temperatures and high pressures by fast compression of a test gas mixture. At the end of the compression stroke, the piston seals the mixture in the test section, where the pressure is measured using a piezoelectric transducer (Kistler 6045A) with a charge amplifier (Kistler 5010B). The test gas mixture composition is determined using the partial pressures of the mixture components, and mixtures are prepared externally prior to a compression experiment in a dedicated stainless-steel mixing tank equipped with a magnetically-driven stirrer. All reactant mixtures used high purity gases and liquids (Sigma

Aldrich;  $\geq 99\%$  cis-2-hexene, 97% cis-3-hexene). The component pressures were measured using a pressure transducer (MKS High Accuracy Baratron Type 690A, accuracy of 0.12% of full scale). All mixtures used fixed equivalence ratios ( $\phi = 1.0$ ) and dilution where Inert gas: $O_2 = 7.5:1$  (molar basis). Nitrogen and argon were used as the inert gases in this study. Mixture compositions for all experiments are provided in the Supplemental Material.

Ignition imaging and gas-sampling and gas-chromatography (GC) analysis were used in the study. Imaging and gas-sampling were not used simultaneously, as both require end-wall access to the RCF. A detailed description of the imaging approach, the gas-sampling system and the GC methodology can be found in Wagnon et al. [13]. A brief summary is provided here. For the end-view imaging, a polycarbonate end-wall allowed optical access to the test section during the experiments. A high-speed color camera (Vision Research Phantom v711) equipped with a fast 50 mm lens (f/0.95, Navitar) with a c-mount extension tube was used to record chemiluminescence that occurred during ignition through the end-wall. Experiments were recorded with a fixed exposure time of 38  $\mu s$  and a rate of 25,000 frames per second.

For the sampling experiments, the transparent end-wall was replaced with a steel end-wall equipped with the gas sampling system. For each sampling experiment, small amounts ( $4.5 \pm 0.5$  mL) of gases were rapidly ( $< 2.5$  ms) withdrawn from the core region of the test section during the ignition delay period. A series of experiments which targeted the same end of compression conditions was used to collect the species data and assemble a composite time history for the measured species. For consistency, the experimental protocol, equipment and GC standard calibration procedure were the

same as used in Wagnon et al. [13], and reproducibility experiments were conducted to confirm the previous results by Wagnon et al. [13].

### 3. Results and Discussion

**3.1 Ignition delay times.** Ignition delay times of cis-2-hexene and cis-3-hexene were measured and compared with the 1-hexene, trans-2-hexene and trans-3-hexene data from Wagnon et al. [13].

Pressure data from typical cis-hexene ignition experiments are presented along with ignition data from the other hexene isomers in **Fig. 2**. All data presented in **Fig. 2** were from experiments at approximately the same state conditions, and the end of compression was set as time  $t = 0$  ms for each. Thermodynamic state conditions and the ignition delay time for each experiment were defined as in Wagnon et al. [13], where the pressure is the time-averaged value from the end of compression ( $P_{\max}$ ) to the maximum in the pressure derivative ( $(dP/dt)_{\max}$ ). Temperature was calculated from the pressure data using isentropic relations, as in Wagnon et al. [13]. The ignition delay time is the time interval between  $P_{\max}$  and  $(dP/dt)_{\max}$ , as shown in **Fig. 2** for cis-3-hexene.

For all the isomers, the compression process was smooth with no irregularities in the pre- or post-compression pressure data. None of the isomers exhibited pre-ignition heat release, i.e. two stage ignition behavior, at the range of conditions studied. The data show little difference between the ignition delay times for the respective cis and trans isomers, and overall there was only slight variation in the ignition delay times (from 16 to 23 ms), with the 3-hexene isomers igniting slightly

faster than the 2-hexene isomers, and 1-hexene was the slowest to react. The overall pressure rise and the rate of pressure rise due to ignition were also comparable for all the isomers.

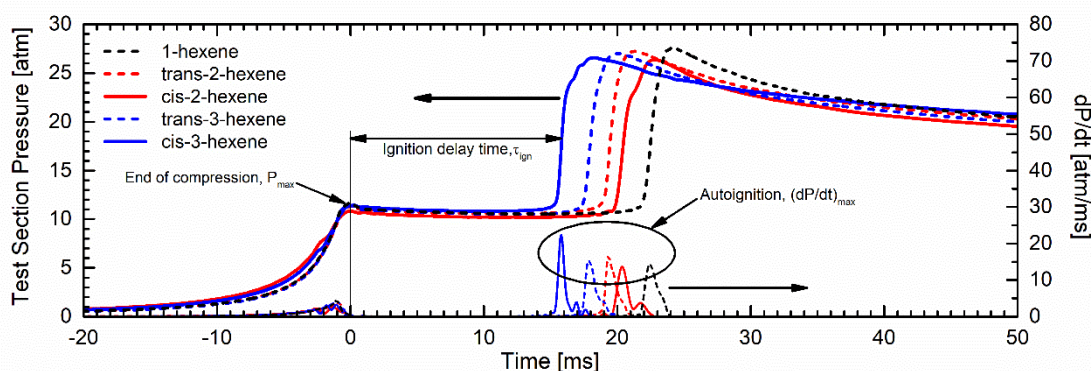


**Figure 2.** Typical pressure and pressure derivative time histories for the five hexene isomers at  $\phi = 1.0$  and  $\text{inert}/\text{O}_2 = 7.5$ . The state conditions for the experiments were approximately the same (1-hexene:  $P = 10.8$  atm,  $T = 900$  K,  $\tau_{\text{ign}} = 22.5$  ms; trans-2-hexene:  $P = 10.8$  atm,  $T = 897$  K,  $\tau_{\text{ign}} = 19.4$  ms; cis-2-hexene:  $P = 10.4$  atm,  $T = 893$  K,  $\tau_{\text{ign}} = 20.4$  ms; trans-3-hexene:  $P = 10.8$  atm,  $T = 896$  K,  $\tau_{\text{ign}} = 17.9$  ms; cis-3-hexene:  $P = 11.1$  atm,  $T = 892$  K,  $\tau_{\text{ign}} = 15.8$  ms). The 1-hexene and trans-hexene data are from Wagnon et al. [13].

**Figure 3** presents frames from the imaging data from the ignition experiments presented in **Fig. 2**. For all isomers, the maximum intensity of the chemiluminescence corresponded with the ignition delay time/the time of maximum pressure rise within 0.3 ms. The imaging data indicate good spatial homogeneity of ignition within the test section and that ignition occurs rapidly and uniformly throughout the test section. Good spatial homogeneity supports the validity of the gas sampling measurements as representative of the overall test gas mixture.

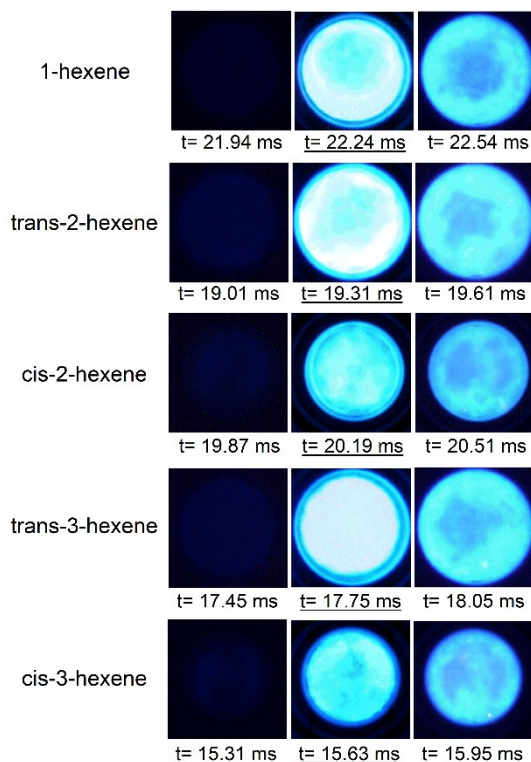


**Figure 3.** Selected frames from the high-speed imaging data corresponding to the pressure–time histories presented in **Fig. 2**. Each frame with the time underlined corresponds to the image with the maximum intensity in the experiment. The 1-hexene and trans-hexene imaging data are from Wagon et al. [13]. The state conditions for the experiments were approximately the same (1-hexene:  $P = 10.8$  atm,  $T = 900$  K,  $\tau_{\text{ign}} = 22.5$  ms; trans-2-hexene:  $P = 10.8$  atm,  $T = 897$  K,  $\tau_{\text{ign}} = 19.4$  ms; cis-2-hexene:  $P = 10.4$  atm,  $T = 893$  K,  $\tau_{\text{ign}} = 20.4$  ms; trans-3-hexene:  $P = 10.8$  atm,  $T = 896$  K,  $\tau_{\text{ign}} = 17.9$  ms; cis-3-hexene:  $P = 11.1$  atm,  $T = 892$  K,  $\tau_{\text{ign}} = 15.8$  ms).

A summary of the measured ignition delay times for the four hexene isomers is presented in the Arrhenius diagram in **Fig. 4**. Experimental conditions for each fuel were fixed at stoichiometric equivalence ratio (based on fuel-to- $\text{O}_2$  ratios) with  $\phi = 1.0$ , and dilution of buffer gas (i.e., inert gas) to  $\text{O}_2$  of 7.5 (molar basis). The ignition delay time data span 809–1052 K with an average pressure of 11 atm. Pressures of specific experiments ranged from 10.1 to 11.5 atm. **Tables S1 - S3** of the Supporting Information include the details of the test conditions and the ignition delay time and

speciation results for the cis-2-hexene and cis-3-hexene experiments. The tabulated results for the 1-hexene, trans-2-hexene and trans-3-hexene experiments can be found in Wagnon et al. [13].

In **Fig. 4**, all data have been scaled to  $P = 11$  atm, using  $\tau_{ign} \propto P^{-1}$ . Error bars in **Fig. 4** represent  $\pm 16\%$  uncertainty and are primarily due to the accuracy of the pressure measurements. The 1-hexene data were within the uncertainty of the other hexene results and are omitted from **Fig. 4** for clarity. The results show the hexene isomers exhibited nearly identical reactivity for the temperature range studied with linear behavior on the log scale. **Figure 4** includes a best-fit regression for all five of the hexene isomers where  $\tau_{ign} = 1.17 \times 10^{-5} \exp(25480 \text{ cal/mol/K})/R_u T$  with an  $R^2$  value of 0.978.

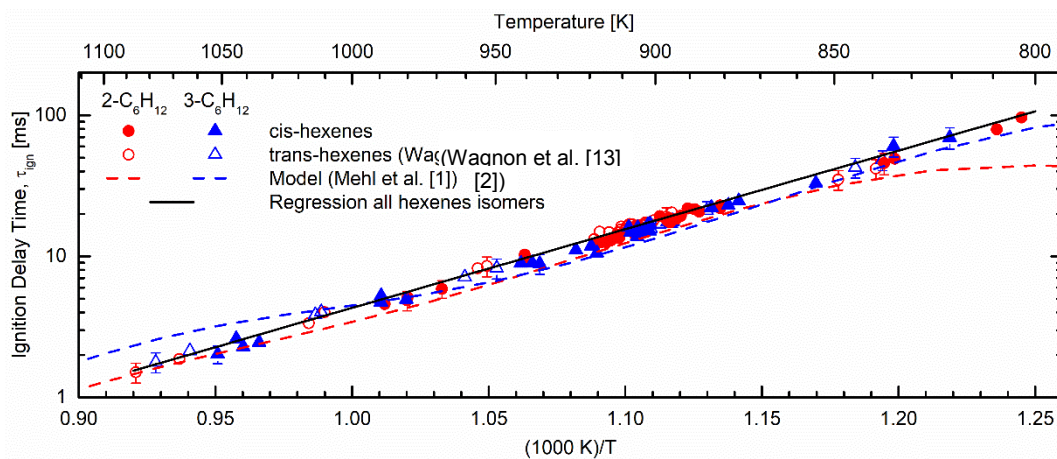


**Figure 4.** Comparison of the hexene isomer ignition delay time measurements. The solid line is a regression for the isomer data. The dashed lines are model predictions using the Mehl et al. [2] reaction mechanism.

**Fig. 4** also shows simulation results (CHEMKIN v10131, x64) for a closed zero-dimensional homogeneous batch reactor with adiabatic and constant volume conditions using the Mehl et al. chemical kinetic mechanism [2]. Average pressure and temperature and the mixture composition from the UM RCF experiments were used as the initial conditions in the 0-D adiabatic constant-volume simulations. The ignition delay time was defined as the time from the start of each simulation to the time corresponding to  $(dP/dt)_{\max}$ . Simulating the compression stroke and an expansion process is sometimes used to represent rapid compression machine experiments. Comparison of the different modeling approaches is shown in the Supplemental Information (**Fig. S1**) for the two cis-hexene isomers. The simulations showed less than 10% difference in the ignition delay times using the different model assumptions for the 3-hexene predictions and negligible differences for the 2-hexene predictions. Hence, all modeling results presented here used constant volume conditions. Additional modeling results (also shown in **Fig. S1**) predict negligible exo- or endothermicity during the ignition delay period before ignition (for the conditions studied), consistent with the experimental observations.

In the Mehl et al. reaction mechanism [2], sub-mechanisms were included for the three linear hexene isomers (1-hexene, 2-hexene and 3-hexene). However, the mechanism did not distinguish between cis- and trans-hexenes. As seen in **Fig. 4**, there is excellent agreement between the simulation results and the experimental data (within the uncertainty of the experimental data) for the temperature range 840 K to 1050 K. Below 840 K, the simulations predict negative temperature coefficient (NTC) behavior starts for 2-hexene, which was not observed experimentally. The work by

Yang et al. [16] for trans-3-hexene predicts NTC behavior below  $\sim 700$  K, which is consistent with the experimental results of this study.

### 3.2 Intermediate Species.

Results from the speciation experiments are shown in **Fig. 5** for the hexene isomers, propanal ( $C_2H_5CHO$ ), propene ( $C_3H_6$ ), acetaldehyde (ethanal,  $CH_3CHO$ ), 1,3-butadiene ( $1,3-C_4H_6$ ) and 1-pentene ( $1-C_5H_{10}$ ). (Results for a pressure time history during a typical gas-sampling experiment, sampling triggering signals, and a typical corresponding chromatogram are provided in the Supplemental Material: **Figs. S2** and **S3**.) The average state conditions for the sampling experiments are  $P = 11.1$  atm and  $T = 911$  K for cis-2-hexene, and  $P = 10.8$  atm and  $T = 903$  K for cis-3-hexene. In **Fig. 5**, the data are normalized to the ignition delay time of the respective experiments (i.e., end of compression corresponds to  $t/\tau_{ign}=0$  and the time of ignition is  $t/\tau_{ign}=1$ ), and the uncertainty in time is defined as the sample interval divided by the ignition delay time. The vertical error bars are the uncertainties in the species measurements, which include repeatability and uncertainty of the GC measurements. When vertical error bars are not visible in the figure panels that indicates the uncertainties were smaller than the size of the symbols on the scale used. Minimum detectivity limits for most species were typically 1 to 10 ppm. . Some smaller features in the chromatograms were not identified and quantified due to the low levels observed and/or challenges with handling the calibration compounds. As with the trans-hexene study, for the majority of the ignition delay period ( $t/\tau_{ign}$  less than  $\sim 0.9$ ), the hexene concentrations and the measured stable intermediates account

for greater than 80% of the carbon initially in the test mixtures. Model predictions calculated using the Mehl et al. mechanism [2] are also shown in **Fig. 5**. The initial conditions for the simulations were the average state conditions of the sampling experiments

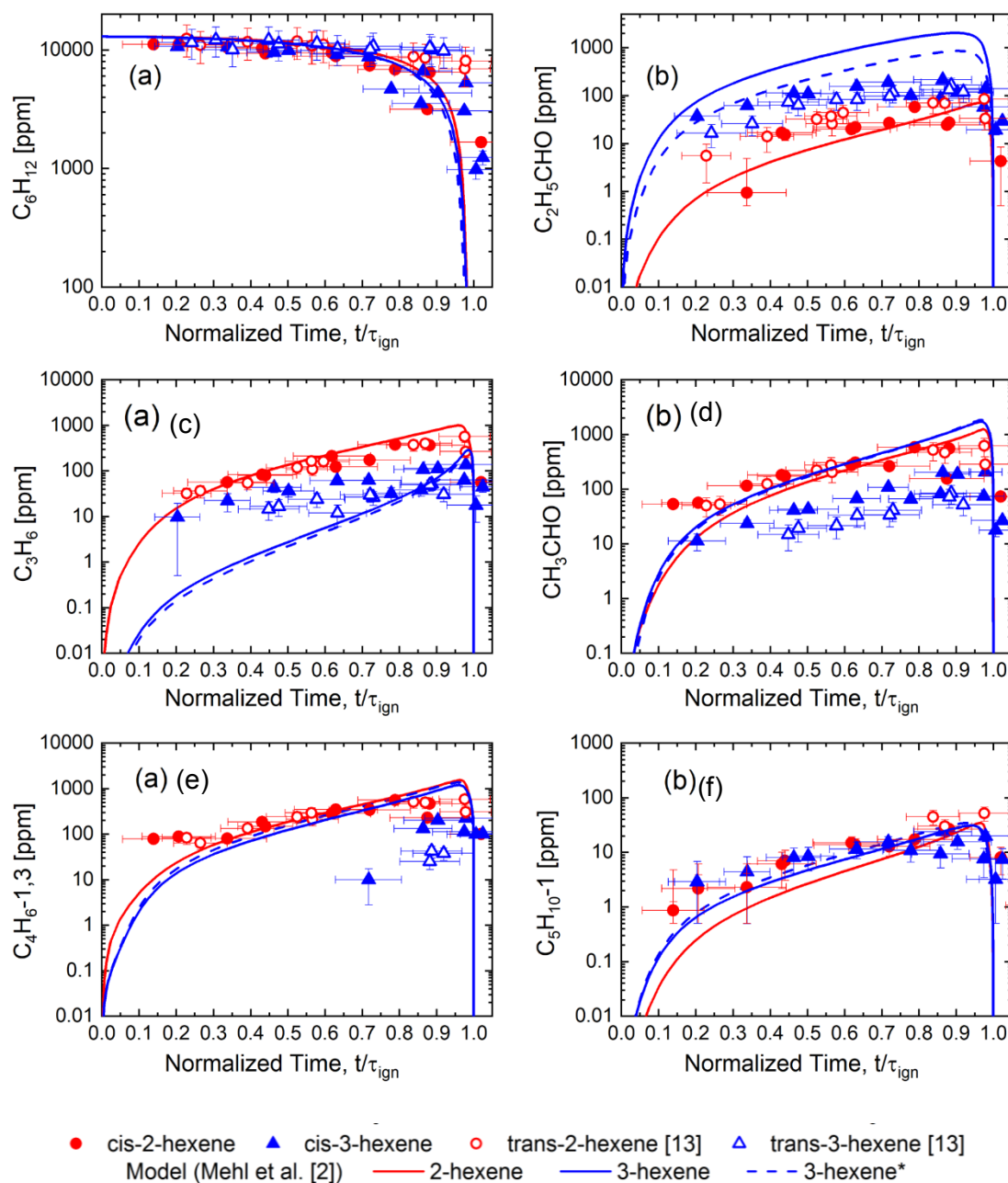


**Figure 5.** Species time histories of (a) hexene isomers, (b) propanal, (c) propene, (d) acetaldehyde, (e) 1,3-butadiene, and (f) 1-pentene during autoignition of the four hexene isomers. Solid lines are predictions using the Mehl et al. mechanism [2]. The state conditions

for the experiments were  $T \cong 900$  K and  $P \cong 11$  atm. The dashed lines are model predictions including revised estimates for the 3-hexene+OH reactions. See text for details.

**Figure 5(a)** presents the time histories of the hexene isomers, and the data show the rates of consumption were nearly identical for all four isomers, until the rapid increase in the rate of consumption near the time of ignition ( $t/\tau_{\text{ign}} > 0.9$ ). Near the time of ignition, the data show the cis-isomers were consumed faster than the trans-isomers. The model is in excellent agreement with the experimental data until later times ( $t/\tau_{\text{ign}} > 0.9$ ), where the model predicts consumption rates more consistent with the experimental trends observed for the cis-isomers.

While the stereoisomeric structure had little effect on propanal production rate as seen in **Fig. 5(b)**, the double bond location did have a systematic effect. The propanal production decreased for cis-2-hexene compared with cis-3-hexene; however, the trend between the trans-hexenes was less clear. On average, the production of propanal from the 3-hexenes exceeded production from the 2-hexenes by  $\sim 5$ -8 times throughout the ignition delay period. For the 2-hexenes, the experimental data and the simulations are in good agreement for cis-2-hexene (within a factor of 2 and generally within the uncertainty of the experimental measurements). However, for the 3-hexenes, the simulations over-predict propanal by more than an order of magnitude.

The experimental data for propene and acetaldehyde also show no obvious differences between the trans-hexene and cis-hexene data for the same double-bond location, as seen in **Fig. 5(c)** and **(d)**. However, for propene and acetaldehyde, the experimental data show the longer alkyl chain (2-hexenes) significantly increased production (by a factor of  $\sim 3.5$ ) compared with production from

the 3-hexenes. The model predicted the propene time histories for 2-hexene very well, and while the model predicted the lower production for propene by 3-hexene, the rate was much lower than observed experimentally (by a factor of  $\sim 4$ ) for times  $t/\tau_{\text{ign}} < 0.6$ . The model predictions for acetaldehyde production from 2-hexene was similarly good; however, the model over-predicted the concentration of acetaldehyde for the 3-hexene isomers by more than a factor of  $\sim 8-10$ .

The results for 1,3-butadiene are presented in **Fig. 5(e)**. The longer alkyl chain significantly promoted 1,3-butadiene production by a factor of  $\sim 10$  higher with the 2-hexenes compared with the 3-hexenes. However, as with the other intermediate species, the cis versus trans structures showed no selectivity to 1,3-butadiene. The simulation results were in good agreement with the 2-hexene data for 1,3-butadiene (generally within the uncertainty of the experimental data for normalized times from 0.25 to 0.8), but the model predicted no preferential production with 2-hexene compared with 3-hexene, which disagrees with the experimental data. Specifically, for the 3-hexene cis and trans data, samples at earlier times ( $t/\tau_{\text{ign}} = 0.5$ ) were below the detectable limit which is around 1 ppm. The model predicts 100 ppm of 1,2-butadiene is formed by  $t/\tau_{\text{ign}} \sim 0.4$  indicating significant over-prediction of 1,3-butadiene at earlier times.

Other measured species, such as 1-pentene (**Fig. 5(f)**), and carbon monoxide, methane, methanol, ethane, ethene, ethyne, 1-butene and methacrolein, presented in **Fig. 6**, demonstrated little sensitivity to the different isomer structures. These species exhibited nearly the same production rates throughout the ignition delay for the four hexenes, and the Mehl et al. [2] mechanism predicted the trends and time histories reasonably well.

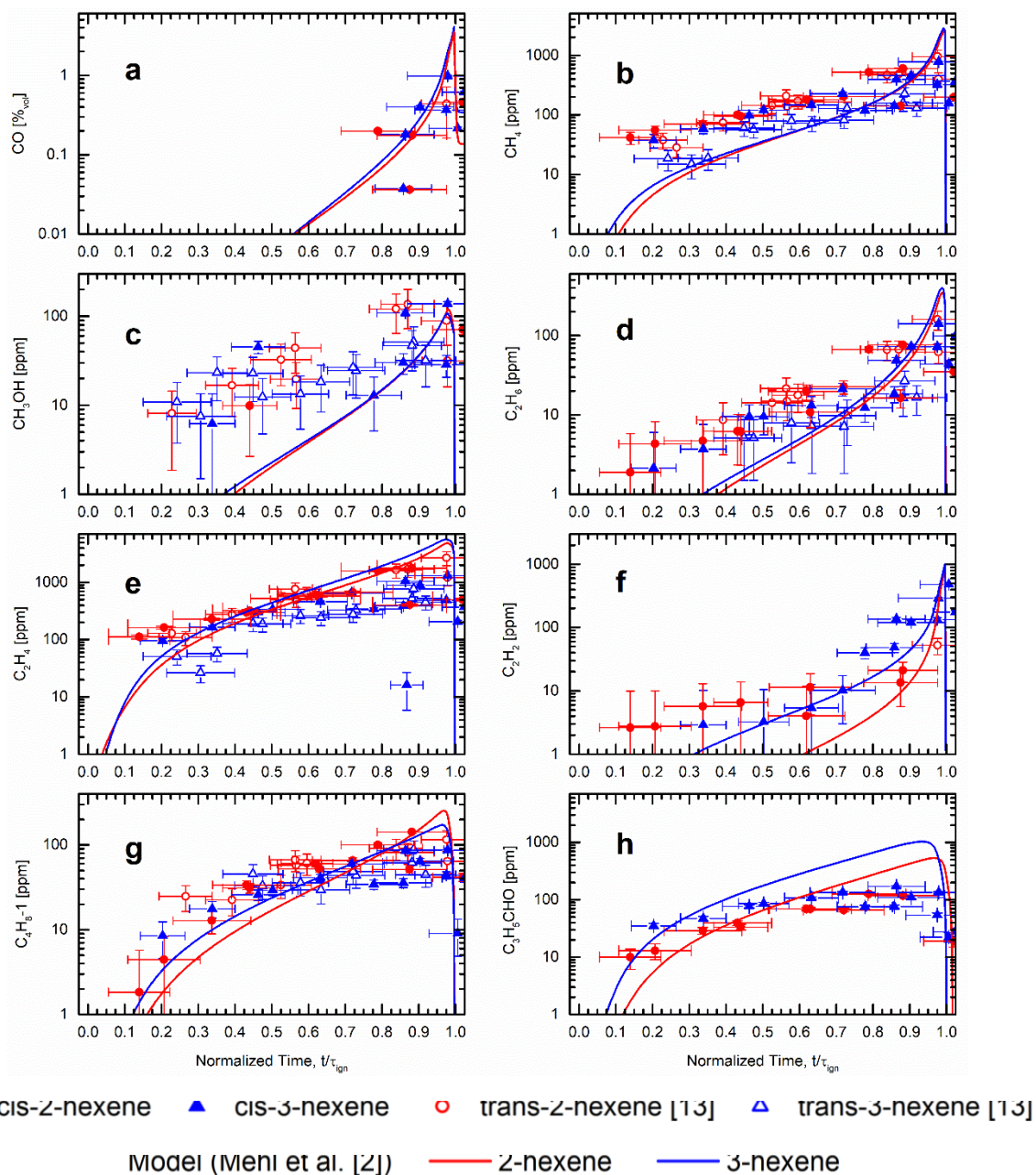


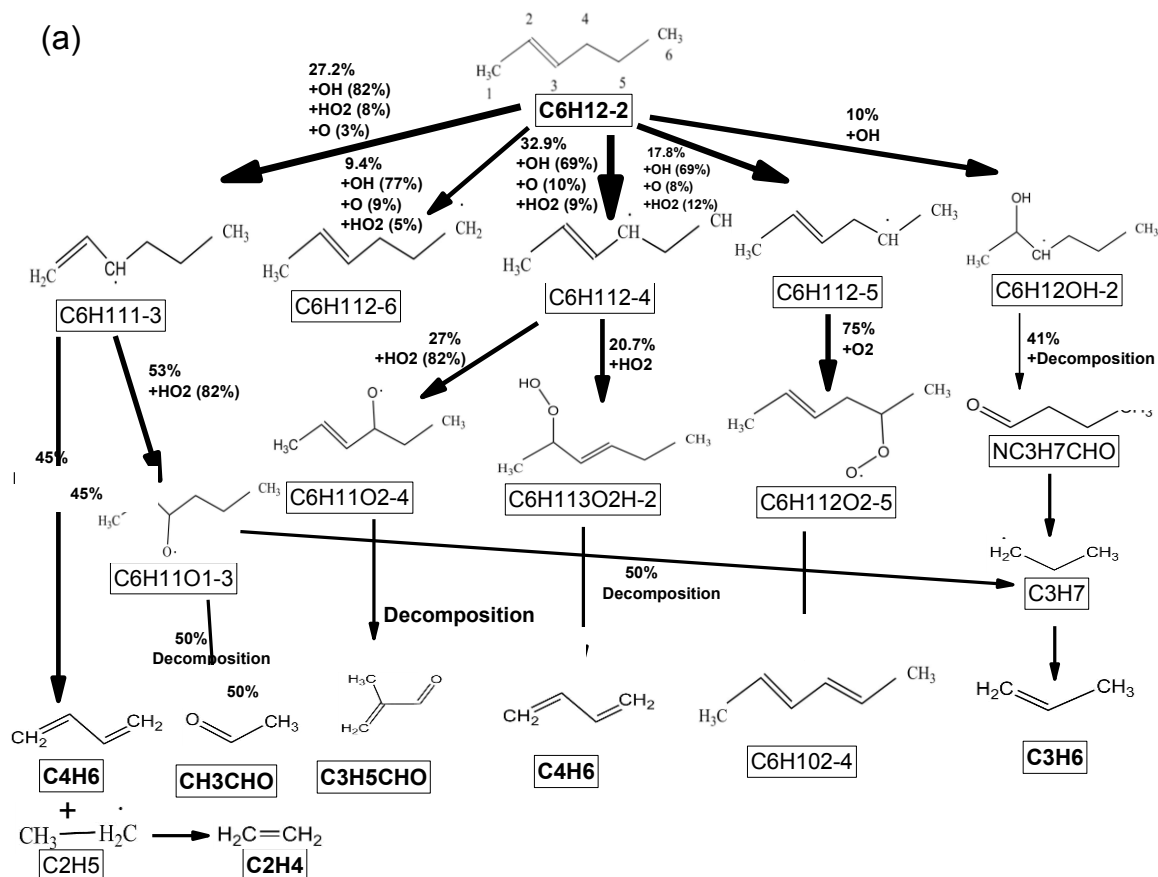
**Figure 6.** Species time histories of a) carbon monoxide b) methane, c) methanol, d) ethane, e) ethene, f) ethyne, g) 1-butene, h) methacrolein. Solid lines are predictions using the Mehl et al. mechanism [2]. The state conditions for the experiments were  $T \cong 900$  K and  $P \cong 11$  atm.

#### 4. Discussion

Reaction path analysis was conducted at the conditions of the sampling experiments to identify the important 2-hexene and 3-hexene reaction pathways. The results are presented in **Fig. 7** at a normalized time of  $t/\tau_{\text{ign}} = 0.9$ . Note that some reaction pathways are “lumped” together in the Mehl et al. [2] reaction mechanism, and the reactions in **Fig. 7** are shown as represented in the Mehl et al. [2] mechanism. Reaction pathways where the arrows are not labeled with collision partners are isomerization, concerted elimination, decomposition, etc. reactions. The reaction path diagram for 3-hexene, which is discussed further below, is based on revised estimates for 3-hexene+OH. In keeping with the original model, H-atom abstraction reactions of the vinylic sites were assumed to be negligible for the mixtures and conditions of this study. H-atom abstraction by OH from the 3-hexene primary carbons was estimated using the linear alkane rate parameters from Sivaramakrishnan et al. [17] with the appropriate reaction path degeneracy (6 “P<sub>1</sub>” hydrogen). An analogy was drawn to 1-butene+OH for the secondary allylic abstractions and the site-specific determination of Vasu et al. [18] was multiplied by 2 to account for twice the secondary allylic hydrogen in 3-hexene. OH-additions to the two equivalent vinylic carbons of 3-hexene were estimated using an analogy to the total (terminal and central) propene+OH addition rate constant from Zador et al. [19].

The reaction path analysis shows the dominant fuel consumption pathway for 2-hexene is by OH abstraction of the H atom, predominantly from the 3 and 4 carbon sites. The various C<sub>6</sub>H<sub>11</sub> radicals formed as products of the H-atom abstraction then react by HO<sub>2</sub> and O<sub>2</sub> addition and by C<sub>6</sub>H<sub>11</sub> decomposition. 3-hexene consumption is also dominated by H atom abstraction by OH; however, predominantly from the 4 carbon site. Yang et al. [14] also conducted reaction path analysis for their

shock tube study of trans-3-hexene. They identified the same reactions as important at  $T = 850\text{ K}$  and  $P = 4, \text{ atm}$ ; however, they also found H atom addition reaction as significant, which was not observed in the current analysis.



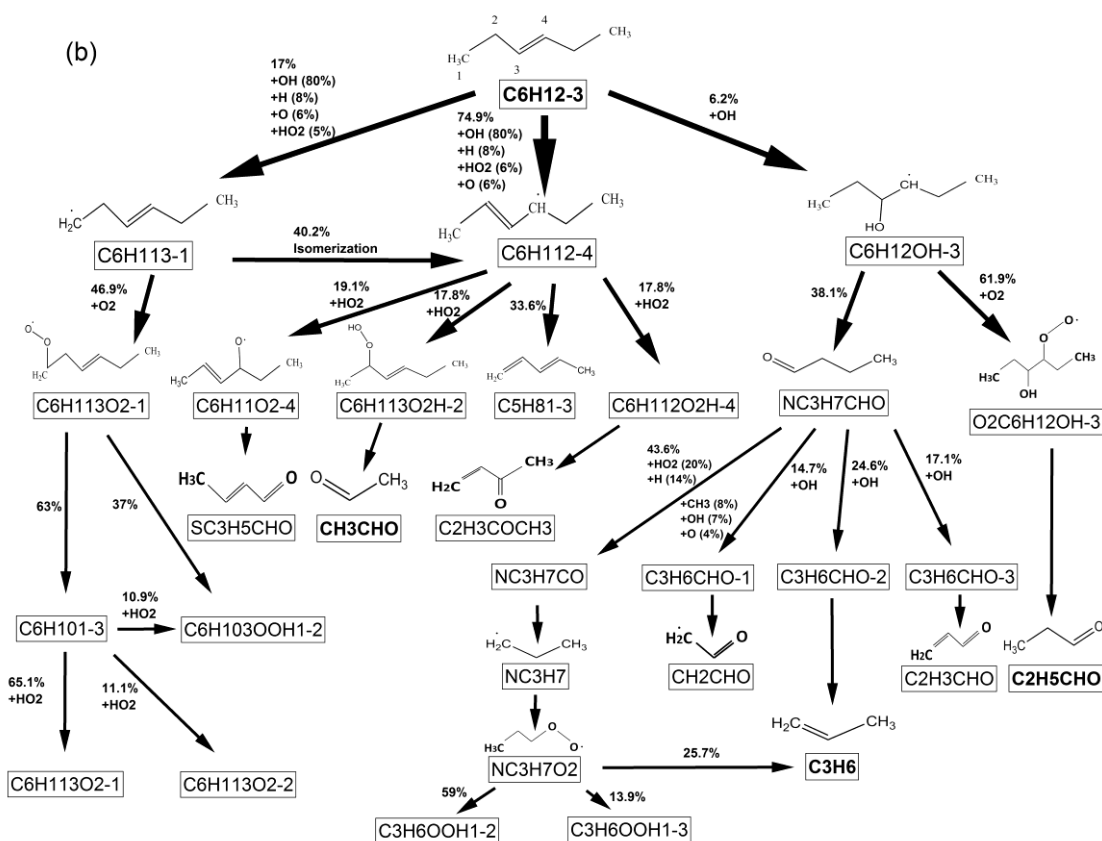
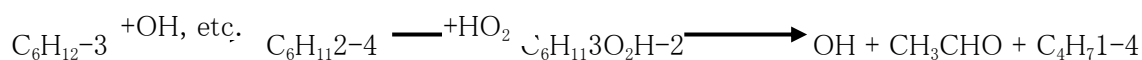


**Figure 7.** Reaction path diagrams for  $T = 900$  K,  $P = 11.0$  atm, and  $t/\tau_{\text{ign}} = 0.9$  based on the Mehl et al. mechanism [2] for (a) 2-hexene and based on the Mehl et al. mechanism [2] with revised estimates for 3-hexene + OH for (b) 3-hexene.

If the mechanism is over-predicting the allylic H-atom abstractions by OH from 3-hexene, it could help explain the over-prediction of acetaldehyde and 1,3-butadiene observed in the current study for the 3-hexene data. However, a second more likely explanation for the over-prediction is also apparent when inspecting the dominant production pathways of acetaldehyde and 1,3-butadiene:

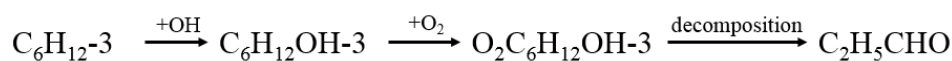


followed by:

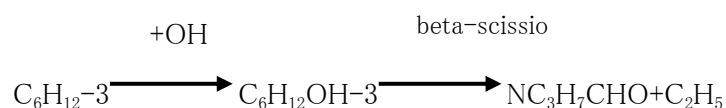


This reaction path sequence is shown, in part, in **Fig. 7**. From the 2-hydroperoxyhex-3-ene ( $\text{C}_6\text{H}_{11}\text{3O}_2\text{H-2}$ ), the Mehl et al. model [2] proceeds through a “lumped” decomposition process to products, which do not appear well justified. Based on previous work studying larger allyloxy decompositions [20], one might reasonably expect the formation of an unsaturated  $\text{C}_5$  aldehyde (e.g., pent-2-enal) in addition to methyl and hydroxyl radicals. None of these products lend themselves to the facile production of acetaldehyde or 1,3-butadiene. Future kinetic models of 3-hexene, which correct this reaction sequence should improve the ability to simulate acetaldehyde and 1,3-butadiene.

Similarly, the under-prediction of propene and over-prediction of propanal ( $\text{C}_2\text{H}_5\text{CHO}$ ) indicates that the 3-hexene+OH and subsequent reactions deserve further consideration. A possibility is that production channels of propene for the 3-hexene system may be absent from the Mehl et al. [2] model. For example, propanal production is dominated by the sequence of reactions ending in Waddington decomposition:

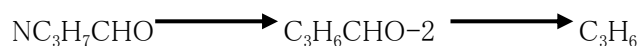


while propene (as shown in **Fig. 7**) is produced mainly by the sequence:

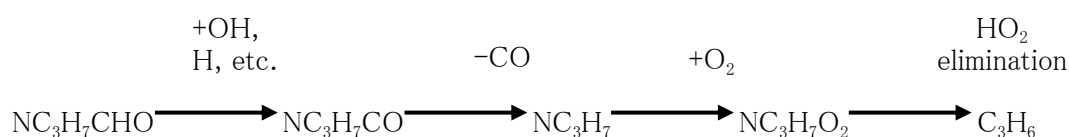


where





and



The ratio of propene production is approximately 4 to 1 for the first to the second of these two reaction sequences. Thus, decreasing the initial 3-hexene+OH addition rate constant to improve agreement with propanal will also decrease the production of  $\text{C}_3\text{H}_6$ , exacerbating the discrepancy with propene. These pathways and their potentially competitive pathways require further discussion.

**Figure 8** illustrates OH addition to 3-hexene and subsequent pathways as currently modeled and potentially competitive pathways that are not in the Mehl et al. [2] model. It is noteworthy that several potentially competitive pathways, for example six-membered isomerizations or concerted  $\text{HO}_2$  eliminations [21], to the Waddington decomposition were not considered in the Mehl et al. mechanism [2]. Inclusion of these pathways may lead to lower simulated concentrations of propanal ( $\text{C}_2\text{H}_5\text{CHO}$ ) in agreement with the current measurements. However, the removal of “lumped” pathways in the model and the addition of detailed beta-scission pathways for  $\text{C}_6\text{H}_{12}\text{OH-3}$  are likely to decrease the simulated concentrations of propene. An initial exploration of this hypothesis was considered here. The “lumped”  $\text{C}_6\text{H}_{12-3}+\text{OH} = \text{PC}_4\text{H}_9 + \text{CH}_3\text{CHO}$  reaction was removed from the Mehl et al. mechanism, and (as described above) analogies were used to estimate new rate coefficients for the  $\text{C}_6\text{H}_{12}\text{OH-3}+\text{OH} = \text{C}_6\text{H}_{11-3-1}+\text{H}_2\text{O}$ ,  $\text{C}_6\text{H}_{12}\text{OH-3}+\text{OH} = \text{C}_6\text{H}_{11-2-4}+\text{H}_2\text{O}$ , and  $\text{C}_6\text{H}_{12}\text{OH-3}+\text{OH} = \text{C}_6\text{H}_{12}\text{OH-3}$  reactions. Note that the rate coefficient recommendations of Yang et al. [16] for  $\text{C}_6\text{H}_{12}\text{OH-3}+\text{OH}$  do not appear consistent in comparison with similar systems, and

consequently were not considered here. The results of the revised mechanism for 3-hexene are presented in **Fig. 5** as the dashed lines. As expected based on this discussion, the model predictions for propanal are improved (with lower levels predicted) while the model predictions for propene are marginally worse (with slightly lower levels predicted). The results show more fundamental consideration of these reactions pathways, beyond the scope of this work, may improve the model predictions to capture the measurements of this study.

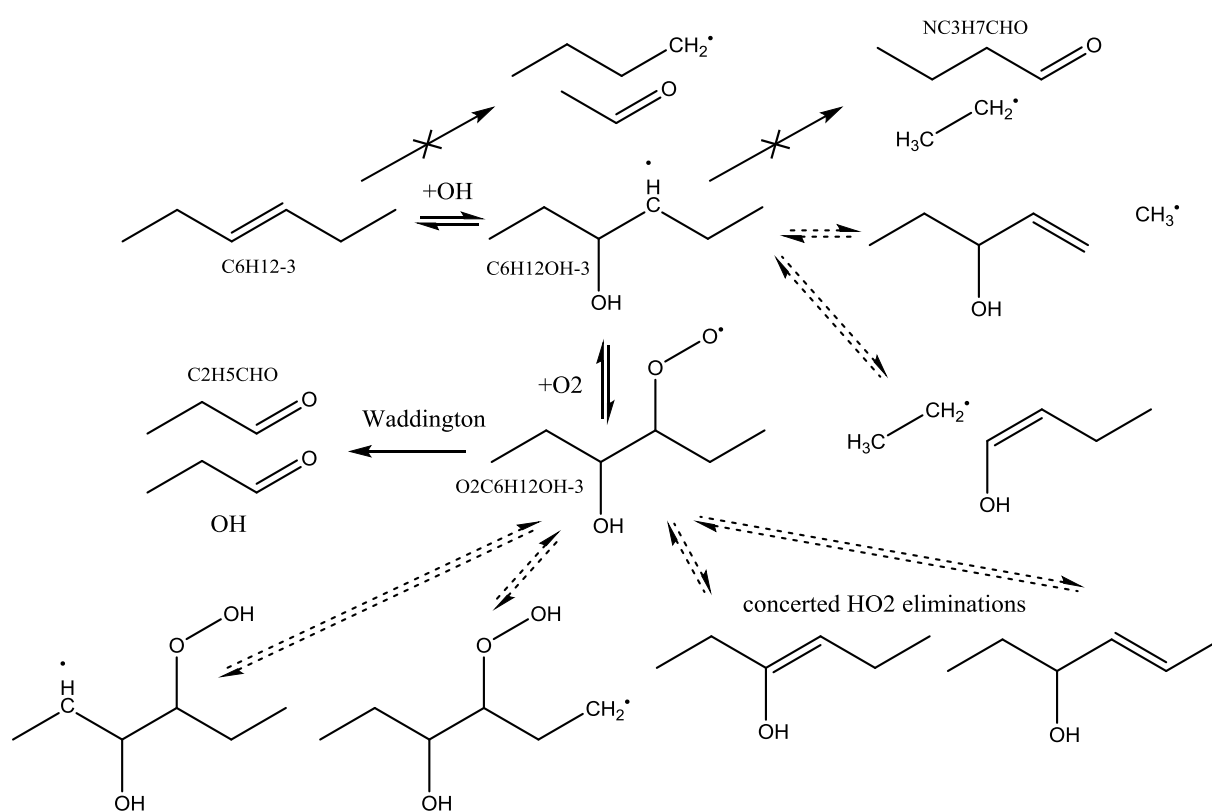


**Figure 8.** Reaction path diagram illustrating existing model pathways (solid arrows) related to OH addition at the C=C double bond in 3-hexene. Potentially competitive pathways (dashed arrows) and the removal of “lumped” pathways (crossed arrows), not currently represented in the reaction mechanism, are also shown.

## 5. Conclusions

By combining new data for cis-hexene ignition obtained in the current work with previous trans-hexene ignition data, the effects of cis/trans hexene isomer structure were considered for the first time at combustion conditions. The results provide key benchmarks for consideration of cis and trans isomer structures on combustion chemistry. The ignition delay time data showed negligible sensitivity to the location of the carbon-carbon double bond or to the stereoisomeric cis-trans structure. However, the intermediate species measurements showed significant differences for the isomer reaction pathways. Specifically, the stereoisomeric (cis-trans) structures had negligible effects on the reaction pathways, based on the species measurements, while the double bond location did alter the reaction pathways. A longer alkyl chain significantly promoted 1,3-butadiene production (by a factor of  $\sim 10$ ) for the 2-hexenes compared with the 3-hexenes, and a longer alkyl chain decreased propanal production by a factor of  $\sim 3$ . Model predictions for ignition delay times were in excellent agreement with the experimental data (within the  $\pm 16\%$  uncertainty of the measurements) and model predictions were in good agreement for many of the intermediate species (e.g., within a factor of 2 for propene during 2-hexene). Key exceptions for 3-hexene included over-prediction of the formation of propanal, acetaldehyde, and 1,3-butadiene and under-prediction at early times of propene for 3-hexene. Additionally, the model predicted stronger selectivity of 3-hexene for propanal compared with 2-hexene than observed experimentally, and the model predicted no 2-hexene selectivity for acetaldehyde and 1,3-butadiene, which was observed experimentally for these species. Evaluation of the model reaction pathways for 3-hexene indicate

fundamental consideration of the 3-hexene+OH and related reactions are a likely source of the observed discrepancies between the model predictions and experimental observations.

## 6. Acknowledgements

The authors acknowledge the support of the US. DOE Basic Energy Sciences via Contract DE-SC0019184, the U.S. DOS Fulbright Program and the Colombian DOSTI-Colciencias, the National Science Foundation Award Number 1701343, and the Department of Mechanical Engineering at the University of Michigan at Ann Arbor. Portions of this work were performed under the auspices of the U.S. DOE by LLNL under Contract DE-AC52-07NA27344.

## 7. References

1. S.K. Hoekman, A. Broch, C. Robbins, E. Cenicerros, M. Natarajan, Review of biodiesel composition, properties, and specifications, *Renew. Sustain. Energy Rev.* 16 (2012) 143-169.
2. M. Mehl, W.J. Pitz, C.K. Westbrook, H.J. Curran, Kinetic modeling of gasoline surrogate components and mixtures under engine conditions, *Proc. Combust. Inst.* 33 (2011) 193-200.
3. C.E.H. Bawn, G. Skirrow, The oxidation of olefins, *Proc. Combust. Inst.* 5 (1955) 521-529
4. W. Tsang, Thermal stability of cyclohexane and 1-hexene, *Int. J. Chem. Kinet.* 10 (1978) 1119-1138.

5. K.D. King, Very low-pressure pyrolysis (VLPP) of hex-1-ene. Kinetics of the retro-ene decomposition of a mono-olefin, *Int. J. Chem. Kinet.* 11 (1979) 1071-1080.
6. M. Yahyaoui, N. Djebaili-Chaumeix, P. Dagaut, C.-E. Paillard, S. Gail, Kinetics of 1-hexene oxidation in a JSR and a shock tube: Experimental and modeling study, *Combust. Flame* 147 (2006) 67-78.
7. X. Fan, G. Wang, Y. Li, Z. Wang, W. Yuan, L. Zhao, Experimental and kinetic modeling study of 1-hexene combustion at various pressures, *Combust. Flame* 173 (2016) 151-160.
8. G. Vanhove, M. Ribaucour, R. Minetti, On the influence of the position of the double bond on the low-temperature chemistry of hexenes, *Proc. Combust. Inst.* 30 (2005) 1065-1072.
9. M. Mehl, G. Vanhove, W.J. Pitz, E. Ranzi, Oxidation and combustion of the n-hexene isomers: A wide range kinetic modeling study, *Combust. Flame* 155 (2008) 756-772.
10. M. Mehl, W.J. Pitz, C.K. Westbrook, K. Yasunaga, C. Conroy, H.J. Curran, Autoignition behavior of unsaturated hydrocarbons in the low and high temperature regions, *Proc. Combust. Inst.* 33 (2011) 201-208.
11. R. Bounaceur, V. Warth, B. Sirjean, P.A. Glaude, R. Fournet, F. Battin-Leclerc, Influence of the position of the double bond on the autoignition of linear alkenes at low temperature, *Proc. Combust. Inst.* 32 I (2009) 387-394.

12. F. Battin-Leclerc, A. Rodriguez, B. Husson, O. Herbinet, P.A. Glaude, Z. Wang, Z. Cheng, F. Qi, Products from the oxidation of linear isomers of hexene, *J. Phys. Chem. A* 118 (2014) 673-683.
13. S.W. Wagnon, C.L. Barraza-Botet, M.S. Wooldridge, Effects of bond location on the ignition and reaction pathways of trans-hexene isomers, *J. Phys. Chem. A* 119 (2015) 7695-7703.
14. F. Yang, F. Deng, P. Zhang, Z. Tian, C. Tang, Z. Huang, Experimental and kinetic modeling study on trans-3-hexene ignition behind reflected shock waves, *Energy and Fuels* 30 (2016) 706-716.
15. F. Yang, F. Deng, P. Zhang, E. Hu, Y. Cheng, Z. Huang, Comparative study on ignition characteristics of 1-hexene and 2-hexene behind reflected shock waves, *Energy and Fuels* 30 (2016) 5130-5137.
16. F. Yang, F. Deng, Y. Pan, Y. Zhang, C. Tang, Z. Huang, Kinetics of hydrogen abstraction and addition reactions of 3-hexene by  $\dot{\text{O}}\text{H}$  radicals, *J. Phys. Chem. A* 121 (2017) 1877-1889.
17. R. Sivaramakrishnan, J.V. Michael, Rate constants for OH with selected large alkanes: shock-tube measurements and an improved group scheme, *J. Phys. Chem. A* 113 (2009) 5047-5060.
18. S.S. Vasu, L.K. Huynh, D.F. Davidson, R.K. Hanson, D.M. Golden, Reactions of OH with butene isomers: measurements of the overall rates and a theoretical study, *J. Phys. Chem. A* 115, (2011) 2549-2556.

19. J. Zádor, A.W. Jasper, J.A. Miller, The reaction between propene and hydroxyl, *Phys. Chem. Chem. Phys.* 11 (2009) 11040–11053.
20. A. Rauk, R.J. Boyd, S.L. Boyd, D.J. Henry, L. Radom, Alkoxy radicals in the gaseous phase: beta-scission reactions and formation by radical addition to carbonyl compounds, *Can. J. Chem.* 81 (2003) 431–442.
21. J.C. Lizardo-Huerta, B. Sirjean, R. Bounaceur, R. Fournet, Intramolecular effects on the kinetics of unimolecular reactions of beta-HOROO\* and HOQ\*OOH radicals, *Phys. Chem. Chem. Phys.* 18 (2016) 12231–12251.